ARL-TM-82-1

AN ANALYSIS OF DEEP OCEAN SOUND ATTENUATION AT VERY LOW FREQUENCIES

Karl C. Focke
Stephen K. Mitchell
Claude W. Horton, Sr.

APPLIED RESEARCH LABORATORIES
THE UNIVERSITY OF TEXAS AT AUSTIN
POST OFFICE BOX 8029, AUSTIN, TEXAS 78712

6 January 1982

Technical Memorandum

Prepared for:

OFFICE OF NAVAL RESEARCH
DEPARTMENT OF THE NAVY
ARLINGTON, VA 22217

UNCLASSIFIED

SECURITY CLASSIFICATION OF THIS PAGE (When Data Entered)

REPORT DOCUMENTATION PAGE	READ INSTRUCTIONS BEFORE COMPLETING FORM
1. REPORT NUMBER	2. GOVT ACCESSION NO. AD-A111 295 / 3. RECIPIENT'S CATALOG NUMBER
4. TITLE (and Subtitle) AN ANALYSIS OF DEEP OCEAN SOUND ATTENUATION AT VERY LOW FREQUENCIES	5. TYPE OF REPORT & PERIOD COVERED technical memorandum
	6. PERFORMING ORG. REPORT NUMBER ARL-TM-82-1
7. AUTHOR(s) Karl C. Focke, Stephen K. Mitchell, Claude W. Horton, Sr.	8. CONTRACT OR GRANT NUMBER(s) N0014-80-C-0490
9. PERFORMING ORGANIZATION NAME AND ADDRESS Applied Research Laboratories The University of Texas at Austin Austin, Texas 78712	10. PROGRAM ELEMENT, PROJECT, TASK AREA & WORK UNIT NUMBERS
11. CONTROLLING OFFICE NAME AND ADDRESS Office of Naval Research Department of the Navy Arlington, Virginia 22217	12. REPORT DATE 6 January 1982
	13. NUMBER OF PAGES 32
14. MONITORING AGENCY NAME & ADDRESS(if different from Controlling Office)	15. SECURITY CLASS. (of this report) UNCLASSIFIED
	15a. DECLASSIFICATION DOWNGRADING SCHEDULE NA

16. DISTRIBUTION STATEMENT (of this Report)

Approved for public release; distribution unlimited.

17. DISTRIBUTION STATEMENT (of the abstract entered in Block 20, if different from Report)

18. SUPPLEMENTARY NOTES

19. KEY WORDS (Continue on reverse side if necessary and identify by block number)

20. ABSTRACT (Continue on reverse side if necessary and identify by block number)

The attenuation coefficient of low frequency, deep ocean acoustic waves is computed for various assumptions regarding the depth profile and the frequency dependence of the scatterers. The calculations are made for a realistic velocity profile by means of a perturbation technique proposed by Guthrie. It is shown that excellent agreement with experimental data is obtained when the attenuation function is independent of frequency and decreases exponentially with depth with a characteristic depth of 200-500 m. A surface value of 0.11 dB/km gives good agreement with the data. At frequencies

DD FORM 1 JAN 73 1473 EDITION OF 1 NOV 65 IS OBSOLETE UNCLASSIFIED

SECURITY CLASSIFICATION OF THIS PAGE (When Data Entered)

20. (Cont'd)

below 50 Hz the attenuation in the water column is comparable to the attenuation in the sediments for the lowest order normal modes.

TABLE OF CONTENTS

LIST OF FIGURES

I. INTRODUCTION

Experimental values of the attenuation of acoustic waves below 100 Hz have steadily accumulated during the last 15 years. Kibblewhite and Hampton[1] have summarized and classified the available data and provided a bibliography. The present report is concerned with the excess attenuation values below 100-200 Hz. Kibblewhite and Hampton introduce a term σ_s, called the scattering coefficient, expressed in dB/km, as a measure of this excess attenuation. Their Table I suggests that this coefficient is related to the water mass in which the acoustic profile is located.

It is not possible at the present time to propose a mechanism for this scattering. Nonetheless, it seems profitable to assign various depth and frequency characteristics to this scattering mechanism and to make quantitative predictions of attenuation for long distance propagation. The results of these calculations will provide significant guidance in the search for and identification of the relevant scattering mechanisms. These calculations extend a line of calculations initiated by Guthrie[2] in his Ph.D. dissertation. Guthrie's work is summarized briefly by Kibblewhite, Shooter, and Watkins[3] in their work on the attenuation of deep water ambient noise.

II. MODELING

This investigation was guided by our experience in computing propagation loss in shallow water propagation. At low frequencies significant propagation loss results from the acoustic energy that propagates in the bottom. Normally this loss would be expected to depend linearly on the frequency.[6] However, the attenuation of clastic sediments varies significantly with the nature of these sediments.[7] Since the lower frequency waves penetrate more deeply, the dependence of propagation loss on frequency may be more strongly influenced by the sedimentary column than by the frequency dependence itself. In any case these considerations suggest that one should not rule out possible depth or frequency distributions on a priori arguments that they are implausible.

The properties of the scatterers in the deep ocean can vary with both depth in the water and frequency. Their effect on the acoustic wave will depend on the variation of the acoustic pressure with depth and thence on the velocity structure of the water and on the mode number of the wave. The following sequence was used in the calculations. After the sound velocity profile was chosen, the eigenfunctions for this velocity structure in the absence of attenuation were computed using the NEMESIS program.[4,5] A specific depth distribution of attenuation was assumed both in the water and in the sediments and the resulting propagation loss was computed by a perturbation technique similar to that used by Guthrie.[2]

Urick[8] has an excellent summary of attenuation in sea water and of the dependence on oceanographic parameters. Figure 1 is a plot of attenuation versus depth based on experimental data of Bezdek[9] and corrected for salinity and temperature variation using formulas by Schulkin and Marsh.[10] This curve shows a maximum attenuation near the

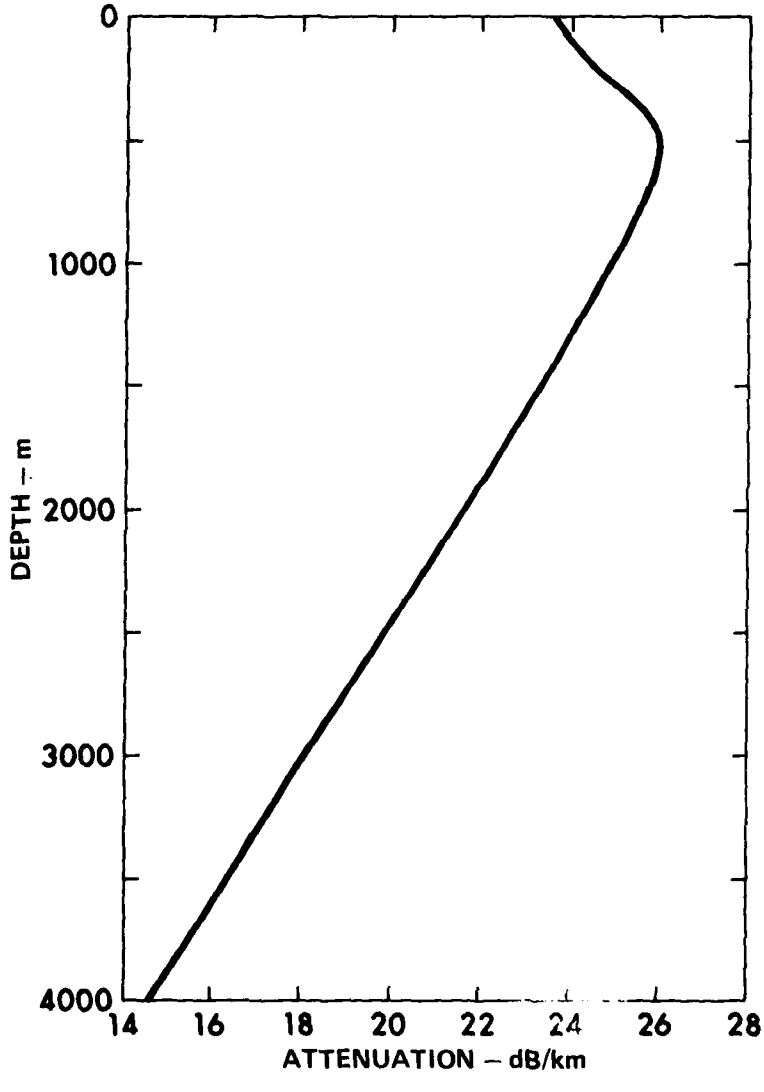

FIGURE 1

ATTENUATION versus DEPTH BASED ON EXPERIMENTAL DATA OF BEZDEK CORRECTED FOR SALINITY AND TEMPERATURE

ARL:UT
AS-81-1070
KCF - GA
8 - 19 - 81

sound channel axis followed by a linear decrease with depth. These curves contrast with the models used in the present analysis where the attenuation is assumed to increase all the way to the surface. This difference is not significant in the near-surface layers since the acoustic pressure vanishes at the surface of the water.

In the models analyzed below, it is assumed that the scatterers are concentrated in the upper 500 m of the water column. This decision was influenced in part by oceanographic data such as the illustrative examples shown in Fig. 2. Mellen and Browning[11] show that pH, and consequently attenuation, in the ocean increases strongly near the sea surface. Another consideration was the amplitude versus depth curves for first order acoustic modes in the deep ocean. Illustrative curves for the amplitude of the first mode for 12.5 and 100 Hz are shown in Fig. 3. These curves illustrate the concentration of the acoustic energy in the upper 1000 m. They also show how the 12.5 Hz mode is more strongly affected than the 100 Hz mode when the attenuation mechanisms are concentrated near the surface of the ocean.

Figures 4 and 5, which are reproduced from Kibblewhite and Hampton,[1] show the phenomena under study. In Fig. 4 the attenuation has a minimum near 60 Hz and appears to increase at lower frequencies. Figure 5 is of interest in that it shows the highest observed values of attenuation at these low frequencies, a result perhaps of the arctic convergence zone.

Figures 6 and 7 provide a visual comparison of the observed attenuations in water and sediments with the boric acid attenuation of Thorp[12] for frequencies of 12.5 and 100 Hz, respectively. It is noteworthy that at 12.5 Hz the attenuation in the water column approaches that of sediments and is greatly in excess of the value for boric acid.

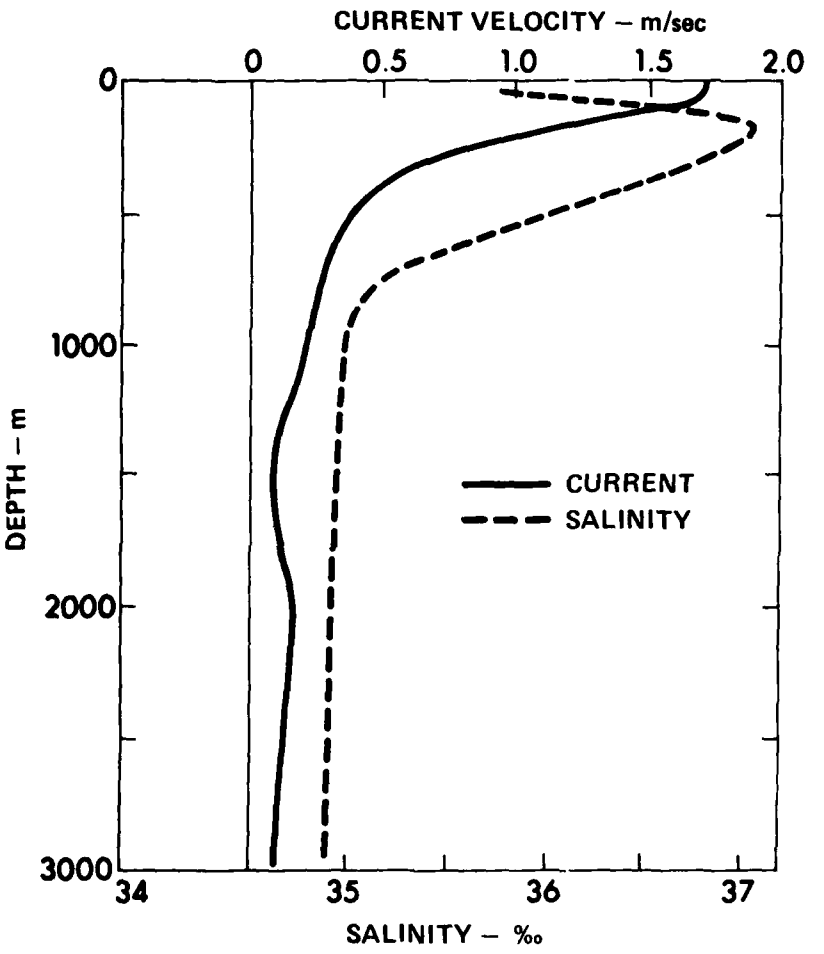

FIGURE 2

TYPICAL DEPTH DEPENDENCE OF CURRENT VELOCITY AND SALINITY

ARL:UT
AS-81-562
KCF - GA
5 - 22 - 81

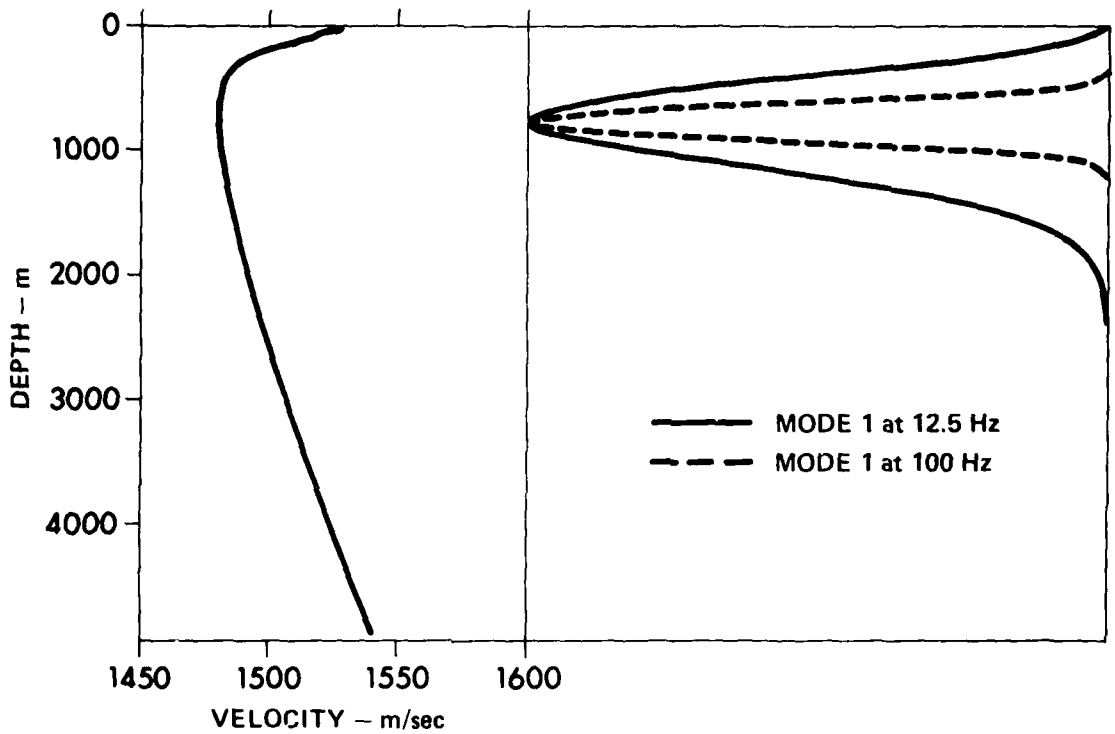

FIGURE 3

ACOUSTIC PRESSURE FOR THE FIRST NORMAL MODE AT 12.5 Hz (SOLID CURVE) AND 100 Hz (DASHED CURVE)

ARL:UT
AS-81-567
KCF - GA
5 - 22 - 81
REV 8-19-81

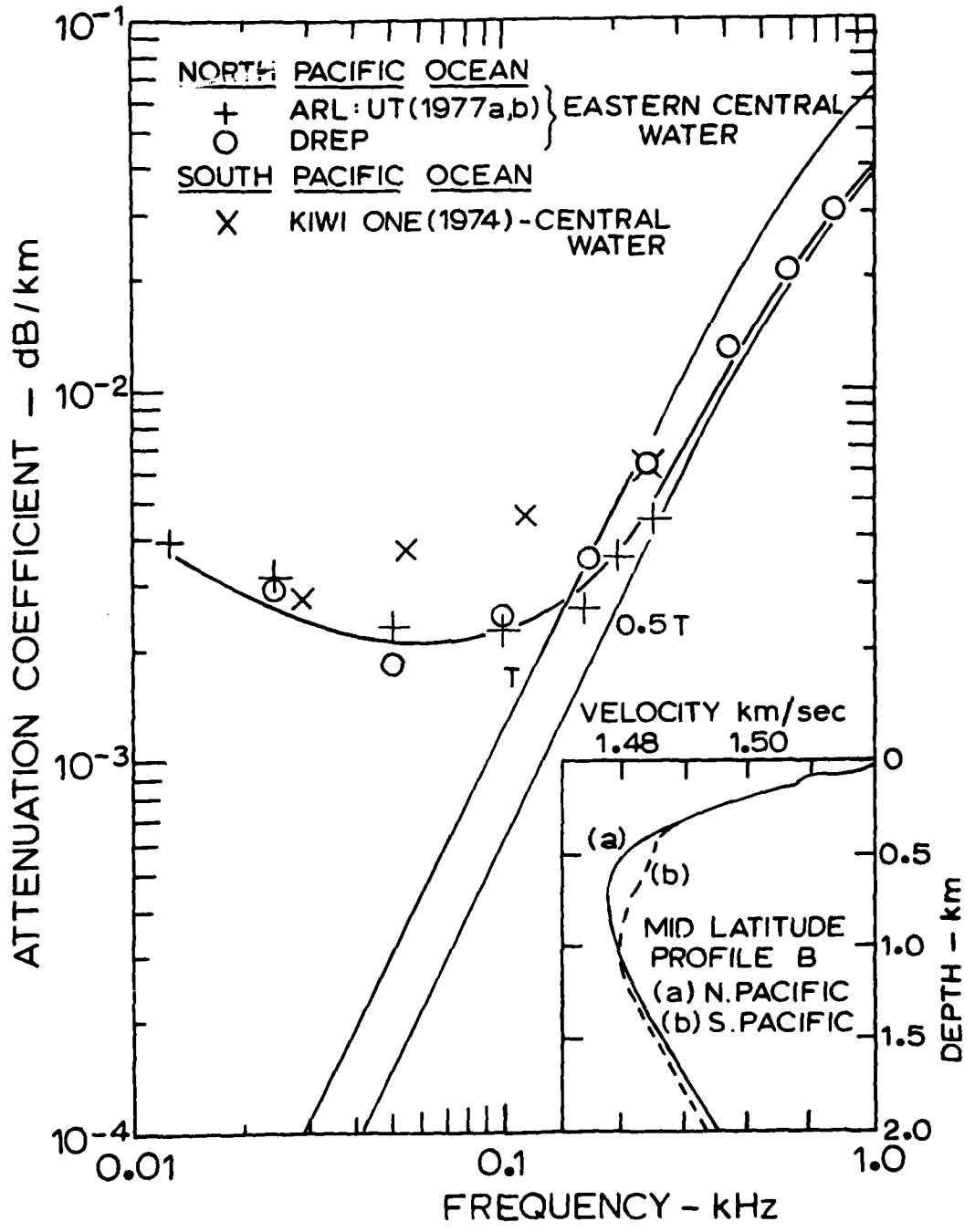

FIGURE 4

ATTENUATION DATA FOR A MID-LATITUDE SOUND VELOCITY PROFILE "TYPE B"

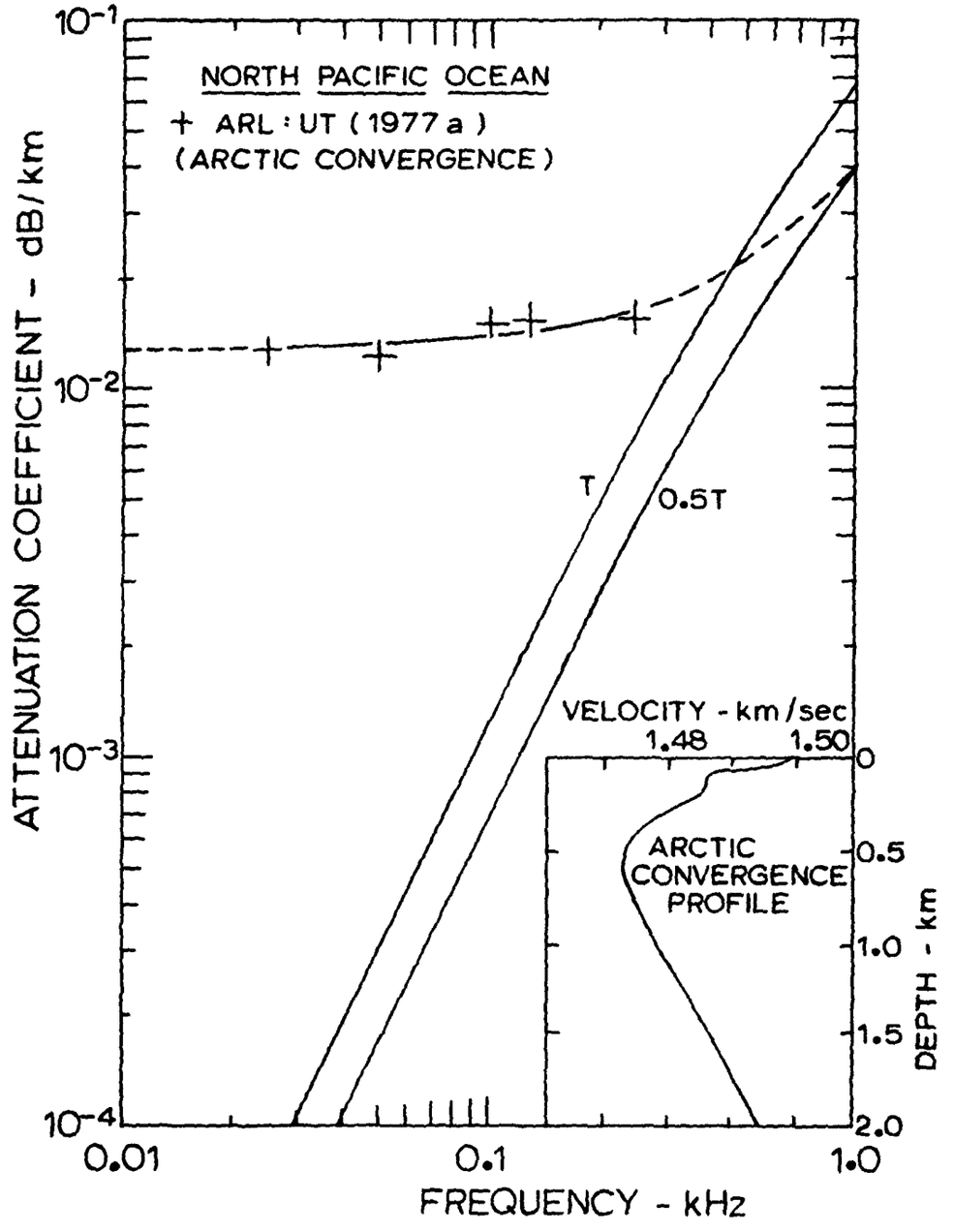

FIGURE 5

AS-78-1607

ATTENUATION DATA FOR THE ARCTIC CONVERGENCE IN THE EASTERN NORTH PACIFIC OCEAN

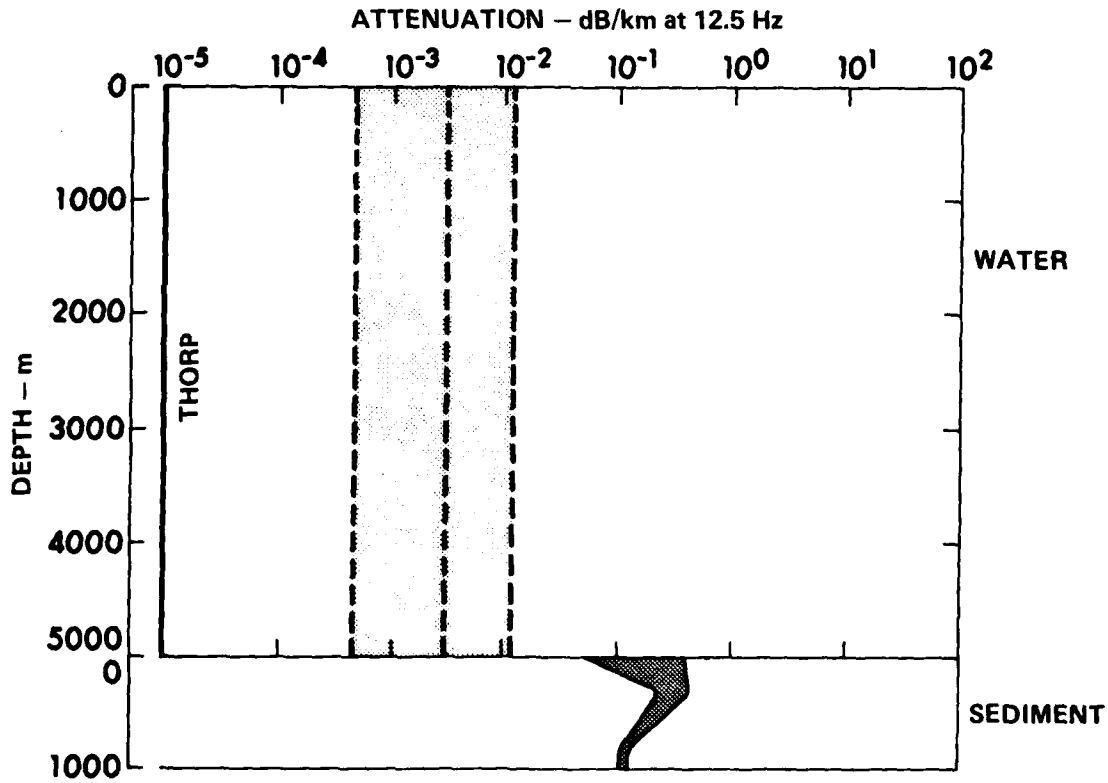

FIGURE 6

COMPARISON OF OBSERVED ATTENUATION AT 12.5 Hz IN WATER AND SEDIMENTS AND THE VALUE PREDICTED BY THE THORP FORMULA

ARL:UT
AS-81-556
KCF · GA
5 · 22 · 81

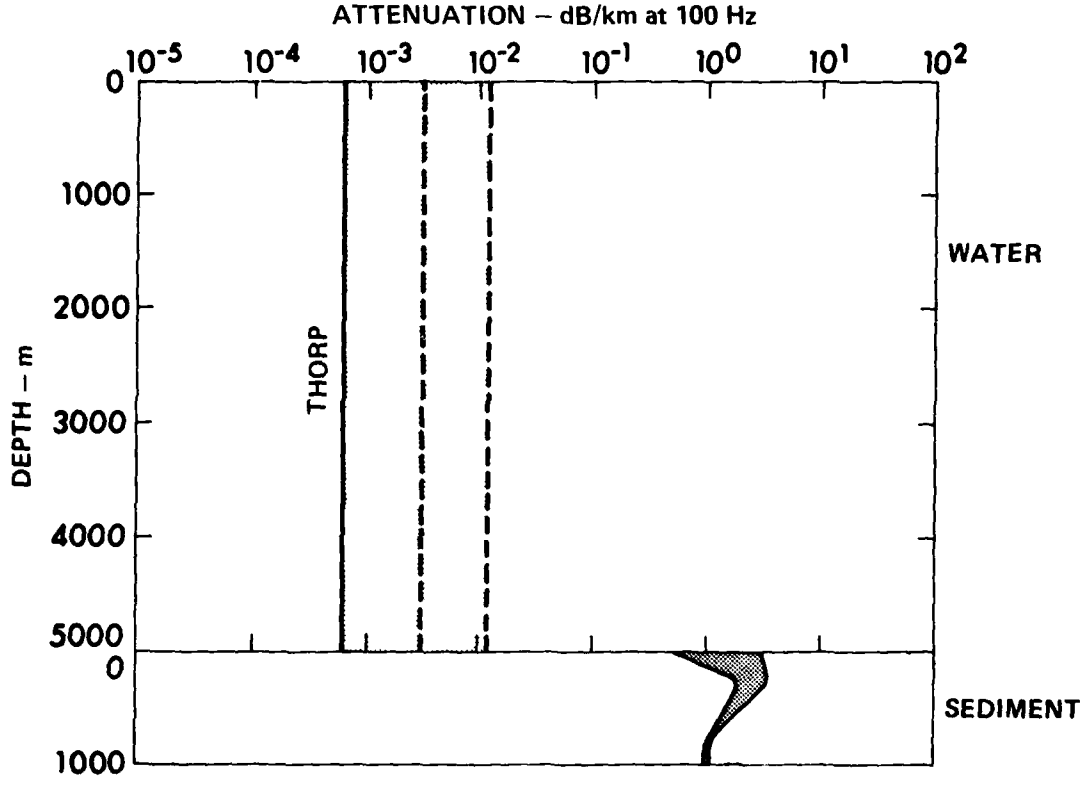

FIGURE 7

COMPARISON OF OBSERVED ATTENUATION AT 100 Hz IN WATER AND SEDIMENTS AND THE VALUE PREDICTED BY THE THORP FORMULA

ARL:UT
AS-81-555
KCF - GA
5 - 22 - 81

III. NUMERICAL PREDICTIONS OF SOUND ATTENUATION

The arguments outlined above suggest a provisional use of the three attenuation profiles shown in Fig. 8. The total attenuation coefficient $\alpha(z,f)$ is the sum of the value $\alpha_T(f)$ predicted by the Thorp curves and the contribution of a frequency dependent profile such as one of those shown in Fig. 8; that is, the attenuation will be computed from the formula

$$\alpha(z,f) = \alpha_T(f) + k(z)f^2 \quad . \tag{1}$$

Figure 9 shows the velocity profile used in the propagation calculations. The water depth is 4883 m. This is underlaid by 50 m of clay. The velocity contrast at the ocean bottom is unity, and the gradient of the sound speed in the sediment is 1.23 sec^{-1}.

As mentioned before, the normal modes are computed first without attenuation, using the NEMESIS program.[4,5] The effect of attenuation, Eq. (1), is introduced by a perturbation technique. These complex normal modes are then used to calculate propagation loss PL(r) at large ranges r. The resulting values of propagation loss are converted to attenuation coefficients with the formula

$$\alpha = (1/2{,}000)\left[PL(1{,}000) - PL(3{,}000) - 10 \log(3{,}000/1{,}000)\right] \quad , \tag{2}$$

which corrects for a cylindrical spreading loss. This method provides a close parallel to the way experimental data are treated.

Figure 10 shows the results of this calculation for profiles I and II of Fig. 8. In each of these curves the surface value of attenuation is 1 dB/km at 100 Hz. The two curves labeled T and 0.5T are the Thorp curves for two different concentrations of boric acid. The

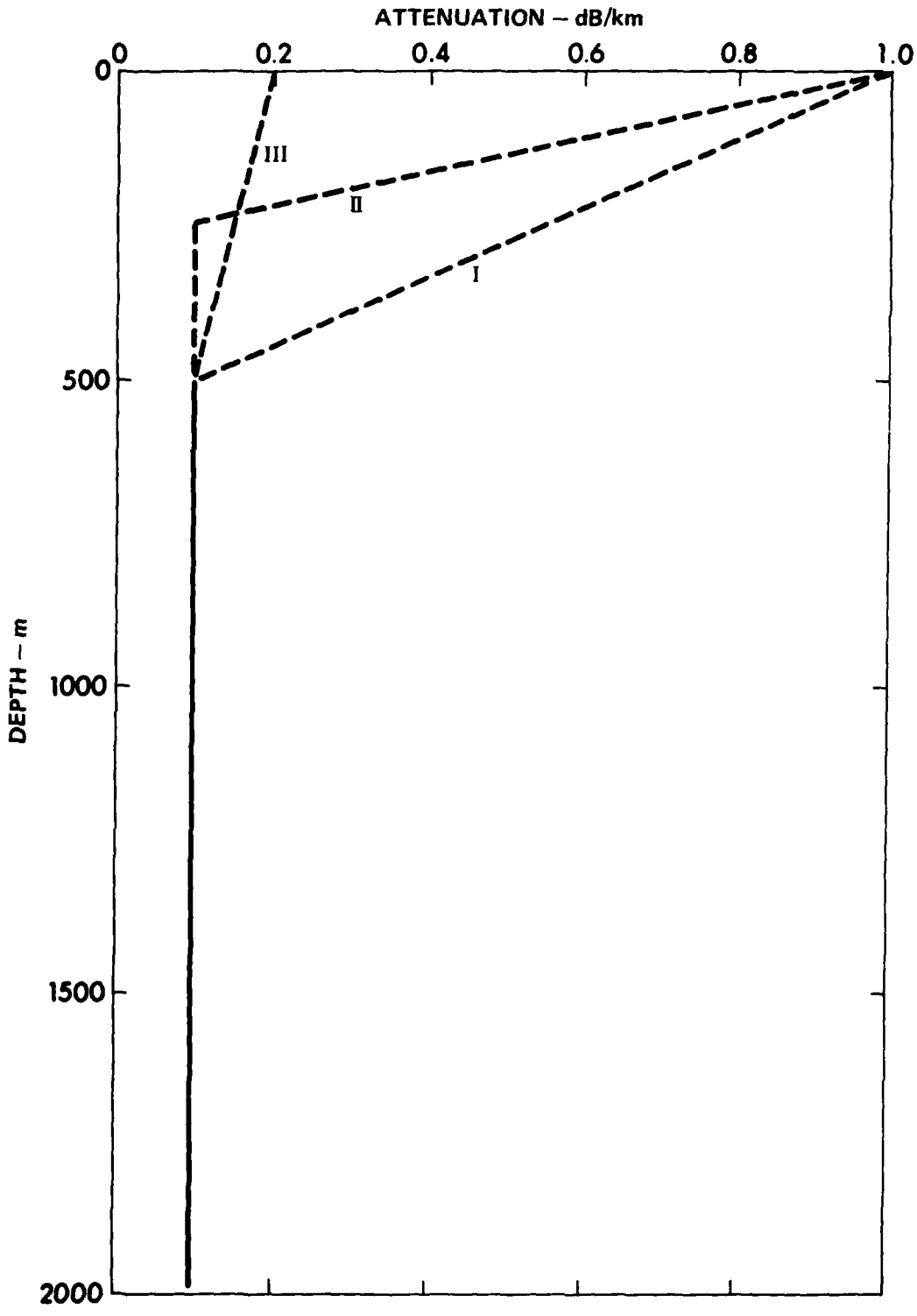

FIGURE 8

THREE ATTENUATION PROFILES USED IN CALCULATING ATTENUATION versus FREQUENCY

ARL:UT
AS-81-678
KCF - GA
6 - 1 - 81

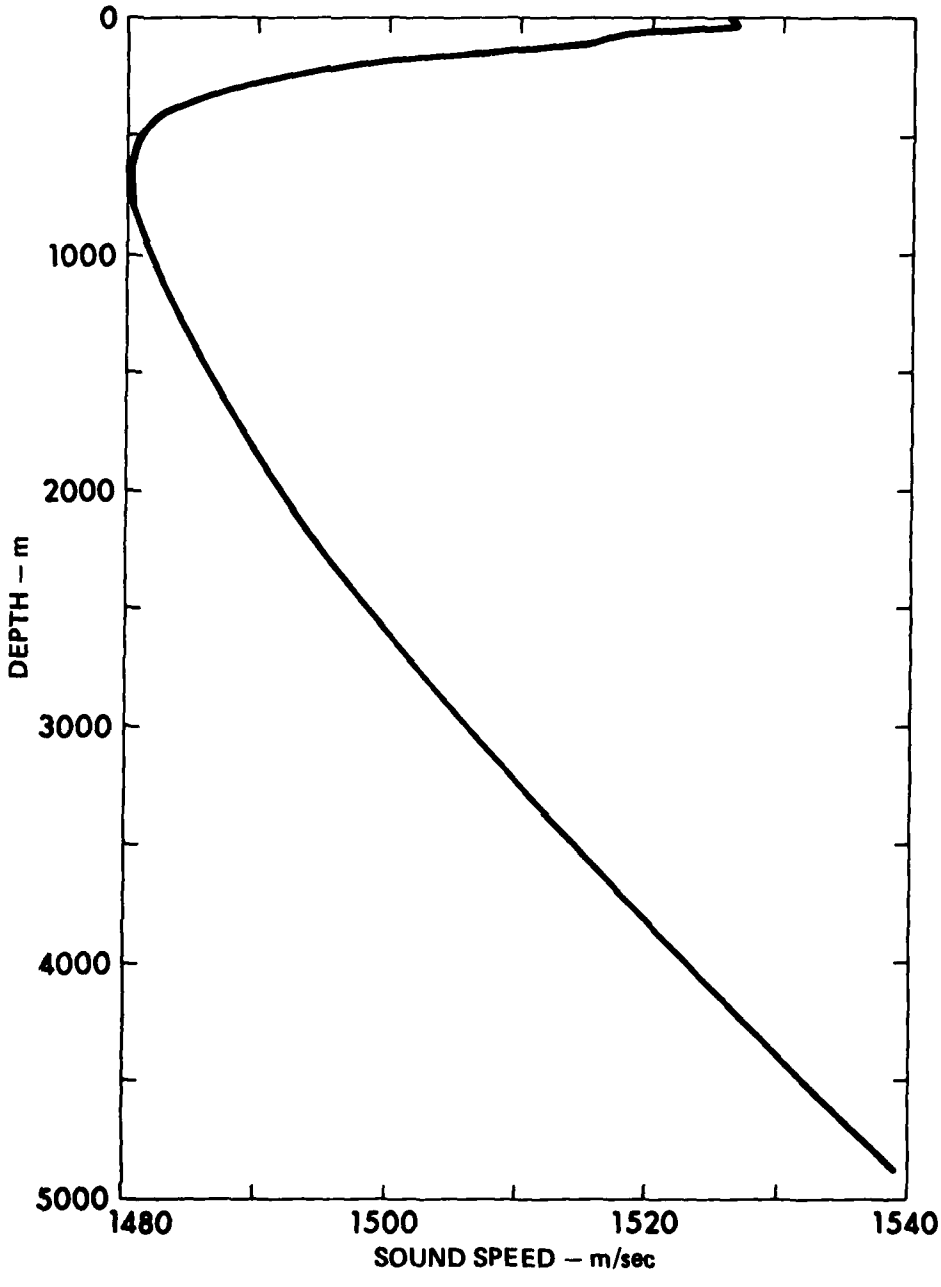

FIGURE 9

THE SOUND VELOCITY PROFILE USED IN CALCULATING ATTENUATION versus FREQUENCY

ARL:UT
AS-81-1036
KCF - GA
8 - 19 - 81

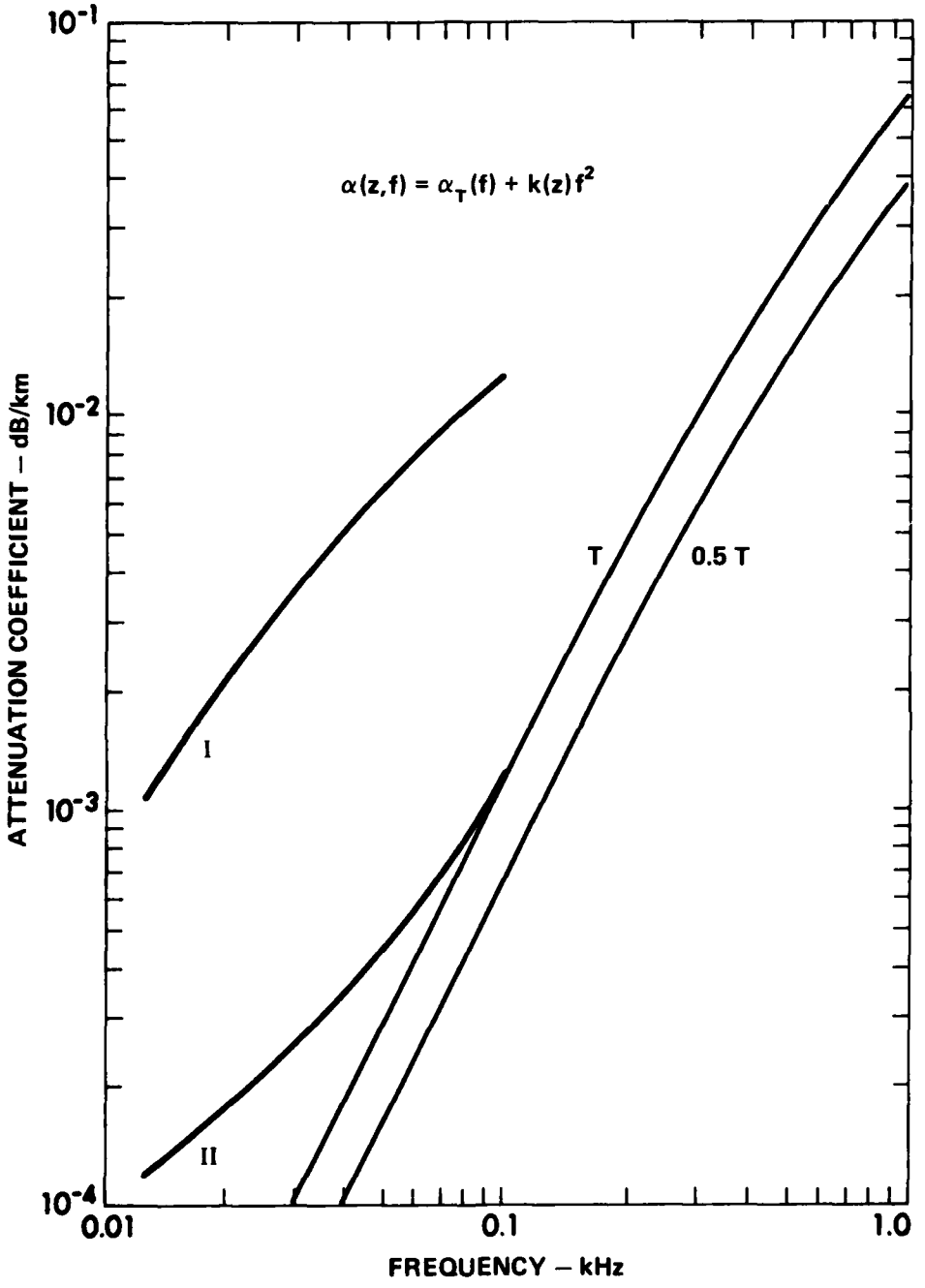

FIGURE 10

CALCULATED COEFFICIENT FOR PROFILES I AND II WITH A FREQUENCY SQUARED DEPENDENCE

THORP CURVES PRESENTED AS A REFERENCE

ARL:UT
AS-81-557
KCF - GA
5 - 22 - 81

attenuation coefficients predicted by these two models and shown in Fig. 10 are not acceptable. Both profiles yield excess attenuation but only profile II shows any flattening at the lower frequencies.

The two curves shown in Fig. 10 are calculated for source and receiver at a depth of 600 m, the depth of the sound channel axis. Since some data are measured with the receiver at a shallower depth, the attenuation coefficient for profile II is repeated with receiver depth at 300 m. Figure 11 shows the results for a source at 600 m and receivers at 300 and 600 m and attenuation profile II. As might be expected the predicted attenuation is larger at 300 m but the frequency dependence has increased. Further calculations with frequency squared attenuation values were made but they did not lead to the flattening of attenuation values observed in the experimental data.

The next set of calculations are based on a formula similar to Eq. (1) except that the frequency factor f^2 in the last term is replaced by f to the first power. These calculations are made with the attenuation profile II of Fig. 8 with three different values of attenuation at z=0. Curves labeled IV, V, and VI correspond to a surface attenuation at 100 Hz of 0.1 dB/km, 0.01 dB/km, and 1.0 dB/km, respectively. The resulting attenuation coefficients, shown in Fig. 12, yield a more nearly satisfactory frequency dependence. Curve VI actually shows a minimum as do some of the experimental curves, but the magnitudes of the theoretical curves are low. It is interesting to note that curve VI of Fig. 12 agrees very closely with the experimental data for a "tropical" sound velocity shown in Fig. 7 of Kibblewhite and Hampton.[1] Figure 13 shows a second calculation of case VI with the receiver located at 300 m in addition to the curve for 600 m. The presence of the minimum is seen to be receiver depth dependent.

As an alternative to the attenuation profiles shown in Fig. 8, the formula

$$\alpha(z,f) = \alpha_o(f) \exp(-z/h) + \alpha_T(f) \quad , \qquad (3)$$

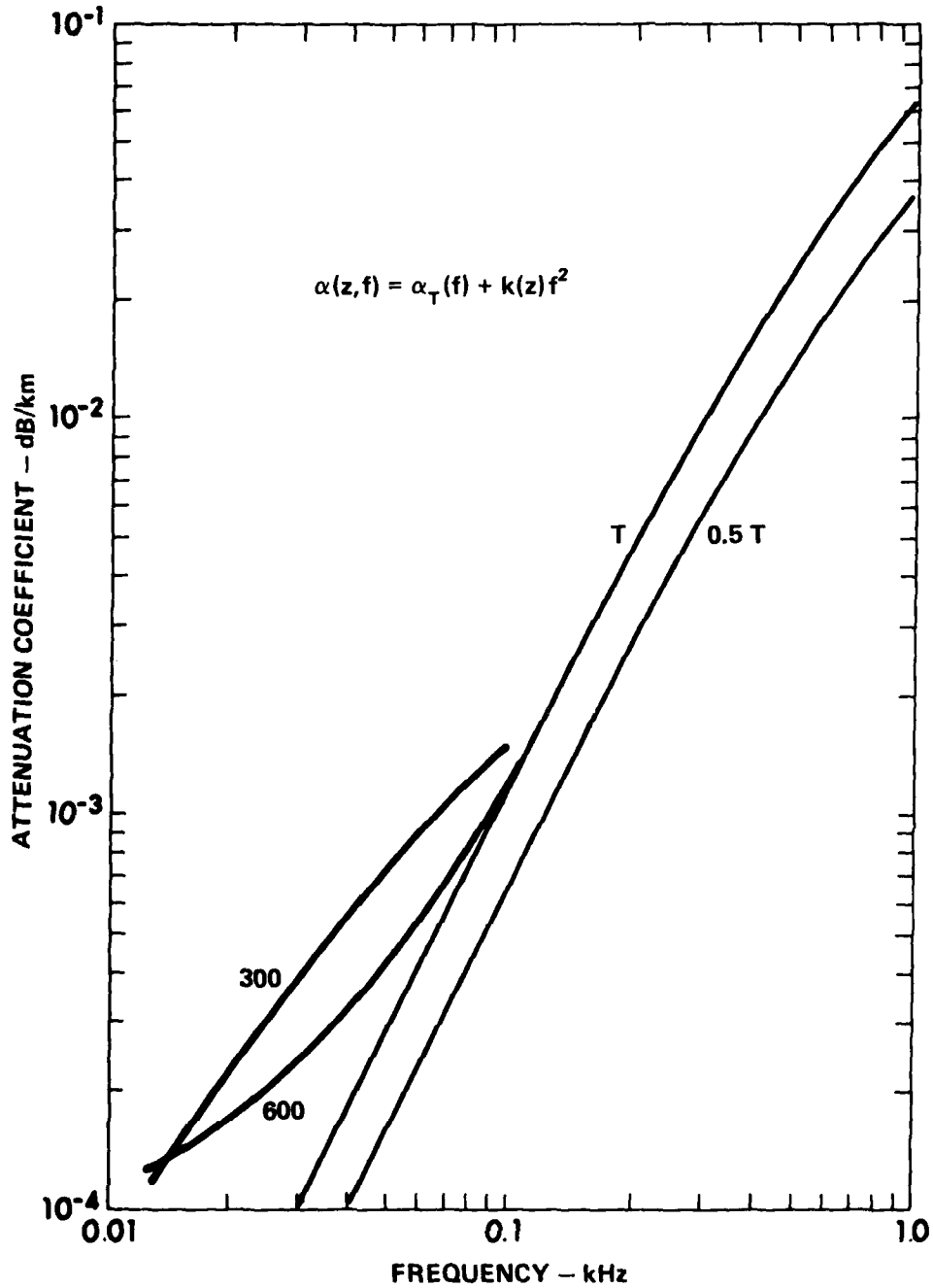

FIGURE 11

EFFECT OF RECEIVER DEPTH FOR PROFILE II WITH A FREQUENCY SQUARED DEPENDENCE

THORP CURVES PRESENTED AS A REFERENCE

ARL:UT
AS-81-558
KCF - GA
5 - 22 - 81

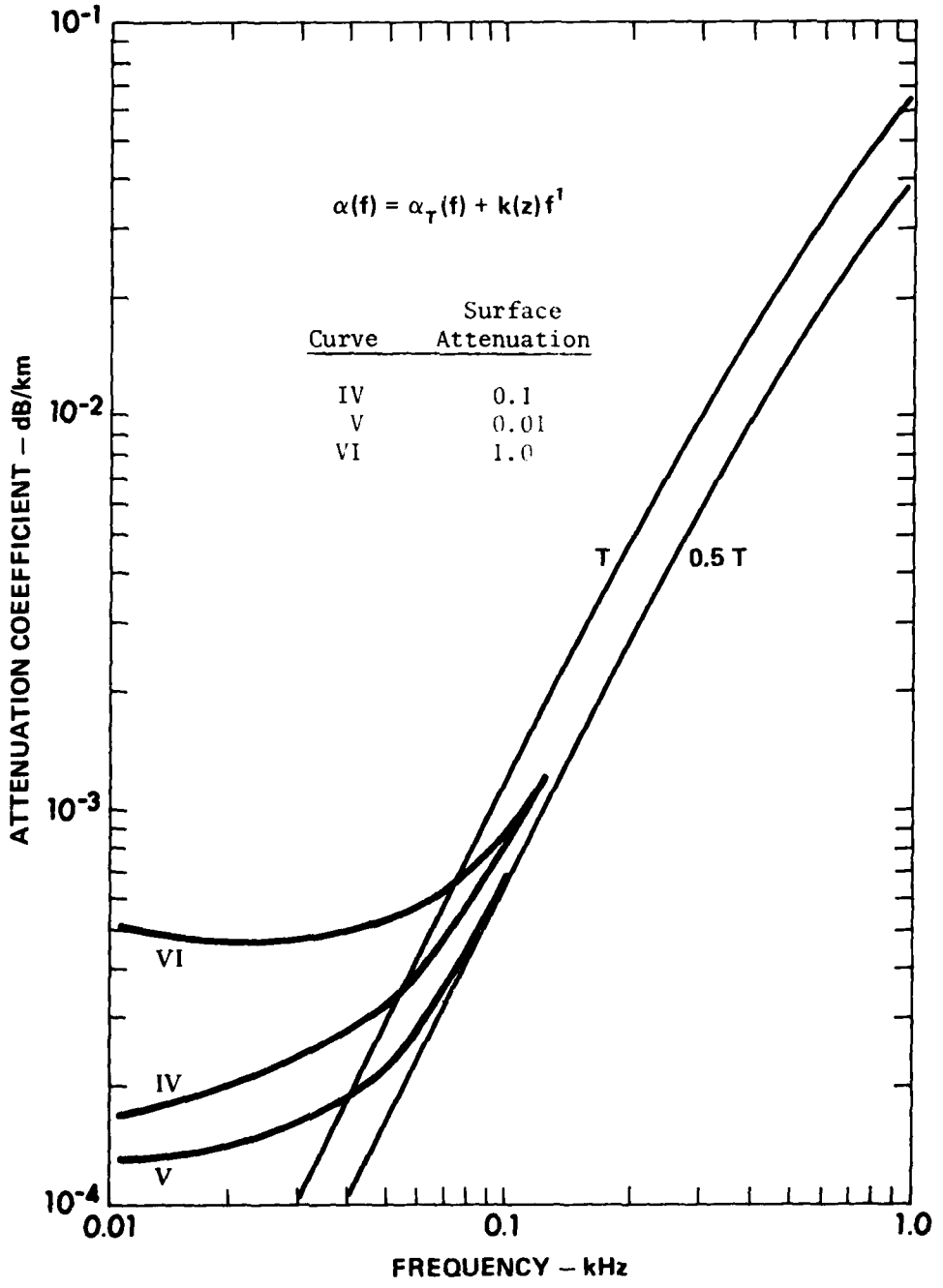

FIGURE 12

CALCULATED ATTENUATION COEFFICIENTS FOR PROFILE II
WITH A LINEAR FREQUENCY DEPENDENCE

ARL:UT
AS-81-559
KCF - GA
5 - 22 - 81

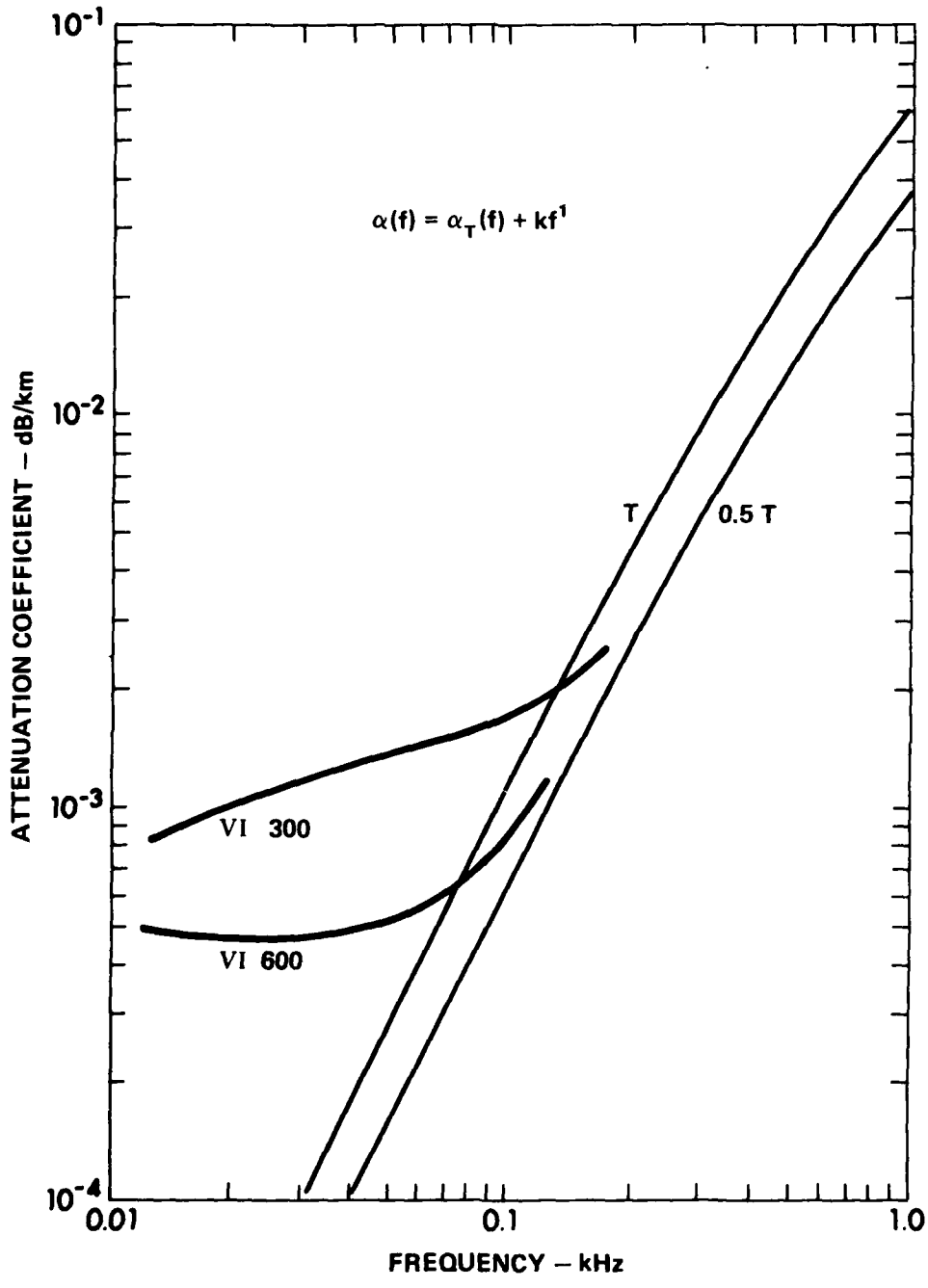

FIGURE 13

DATA SIMILAR TO FIG. 12 FOR RECEIVER DEPTHS OF 300 m AND 600 m

ARL:UT
AS-81-676
KCF - GA
6 - 1 - 81

is tried with h = 200 m and $\alpha_o(f)$ = 0.1(f/100) dB/km where f is in hertz. The two curves shown in Fig. 14, computed for receiver depths of 300 and 600 m, do not show the desired frequency dependence.

The attenuation coefficients, selected to describe a profile, need to be consistent with the measured values at frequencies above 1 kHz and in particular above 10 kHz. Based on the work of Schulkin and Marsh,[10] the surface attenuation value at 10 kHz should be approximately 1 dB/km. The surface attenuation value for a linearly frequency dependent term, necessary in matching the low frequency measurements, would exceed this 10 kHz value by at least an order of magnitude.

The behavior of the attenuation coefficients computed so far forces one to the conclusion that a successful scattering model will be very insensitive to frequency. Consequently the attenuation function of Eq. (3) is tried for the special case $\alpha_o(f)$=constant. This is a model of the attenuation that was proposed and investigated by Guthrie.[2] The three attenuation curves plotted in Fig. 15 are computed for α_o = 0.11 dB/km and for h = 200 m, 250 m, and 500 m. In each case the attenuation has a minimum. The frequency of the minimum increases as the characteristic depth h increases. These curves reproduce rather well the behavior of the experimental data summarized by Kibblewhite and Hampton[1] and the two examples reproduced in Figs. 4 and 5 of the present report. The magnitude of the attenuation in the flat portions of the curves spans very nicely the values of α_s listed in Kibblewhite and Hampton's Table I.

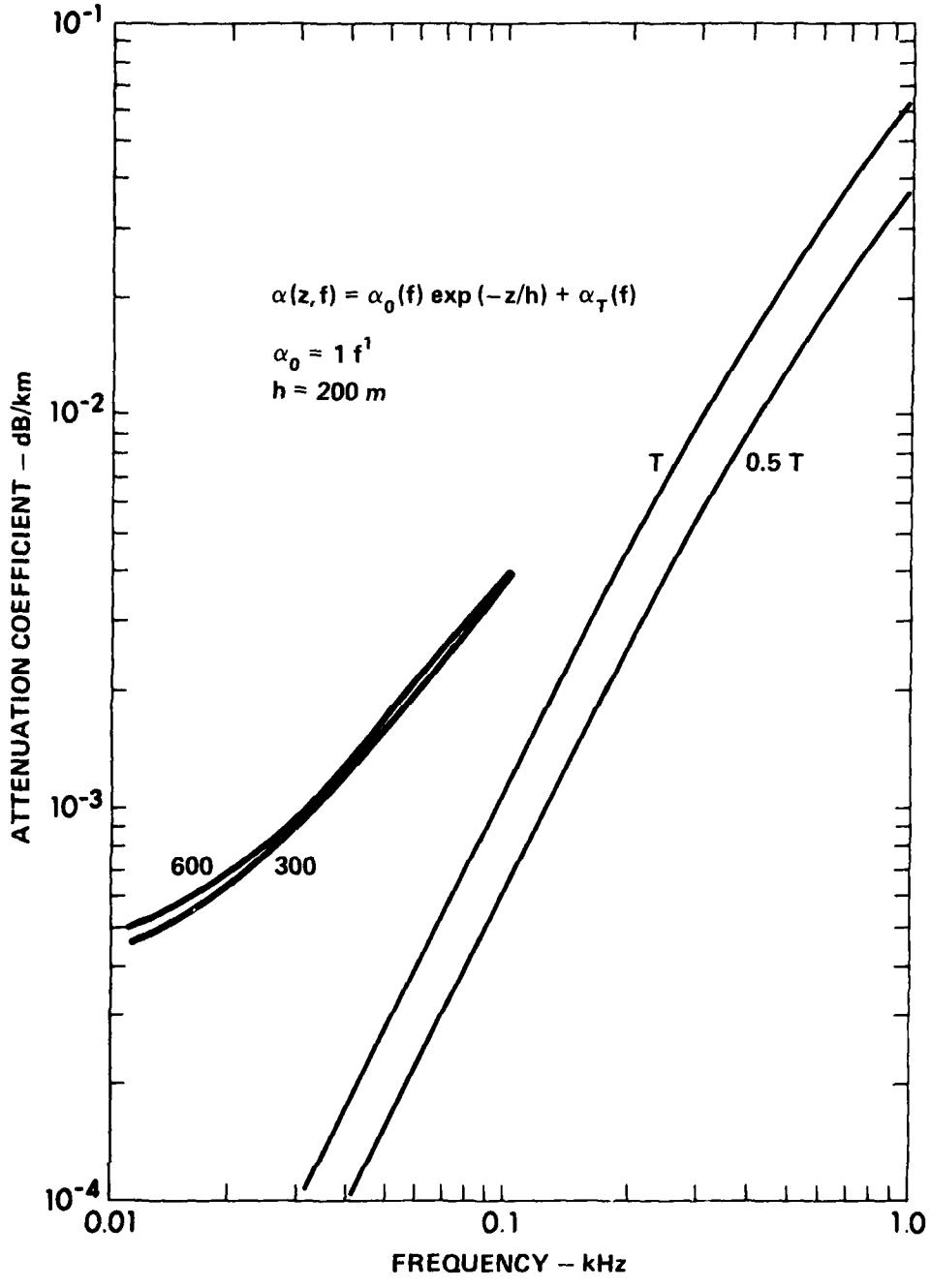

FIGURE 14

CALCULATED ATTENUATION COEFFICIENTS FOR AN ATTENUATION PROFILE WITH AN EXPONENTIAL DEPTH DEPENDENCE AND A LINEAR FREQUENCY DEPENDENCE

RECEIVER DEPTHS AS A PARAMETER

ARL:UT
AS-81-679
KCF - GA
6 - 1 - 81

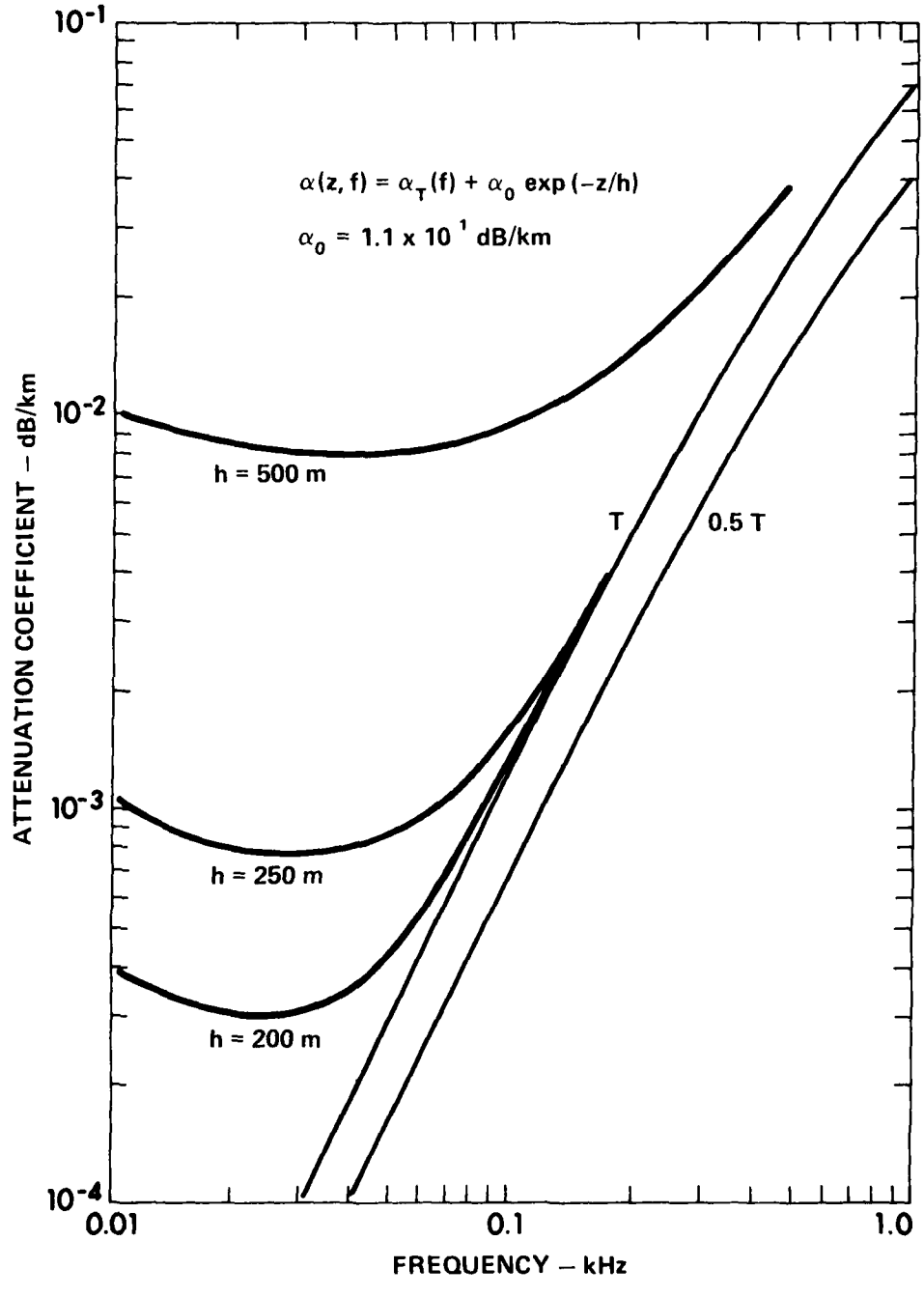

FIGURE 15

CALCULATED ATTENUATION COEFFICIENTS FOR AN ATTENUATION PROFILE WITH AN EXPONENTIAL DEPTH DEPENDENCE AND INDEPENDENT OF FREQUENCY

THE CHARACTERISTIC DEPTH, H, AS A PARAMETER

ARL:UT
AS-81-560
KCF - GA
5 - 22 - 81

IV. COMMENTS

The calculations presented here do not furnish a mechanism for the attenuation of deep ocean acoustic waves, but they do provide a set of quantitative characteristics that any proposed mechanism must fit. In particular the attenuation is localized in the upper 500 m of the water column and it must be very insensitive to frequency. Although the magnitude of the assumed attenuation is small, it does not differ significantly from the attenuation in sediments at these low frequencies. This is illustrated in Fig. 16, where the attenuation used in these models is compared with the experimental data obtained in the last five years for oceanic sediments. These attenuation values are within a factor of ten of each other at 50 Hz. Since the path length in water is often ten times greater than the path length in the sediment for these low order modes, the attenuation produced by the waterborne scatterers has the same magnitude as the attenuation in the sediments.

The path lengths in water and in the sediments are shown in Fig. 17 as a function of bottom grazing angle. These curves are computed for the sound velocity profile shown in Fig. 9 and for a water depth of 4883 m. In these calculations the ocean bottom has 500 m of clay overlying basalt. The velocity contrast between the water and clay is unity and the velocity gradient in the clay is 1.23 sec^{-1}. The path lengths are seen to differ by at least an order of magnitude. As stated above, these differences can offset the differences in the attenuation of the two media, and thus the waterborne scatterers can influence the mode attenuation as much as the sediment attenuation.

In summary it is claimed that the attenuation observed in the deep ocean at frequencies below 100 Hz is produced by frequency independent mechanisms that are concentrated in the upper 500 m of the ocean.

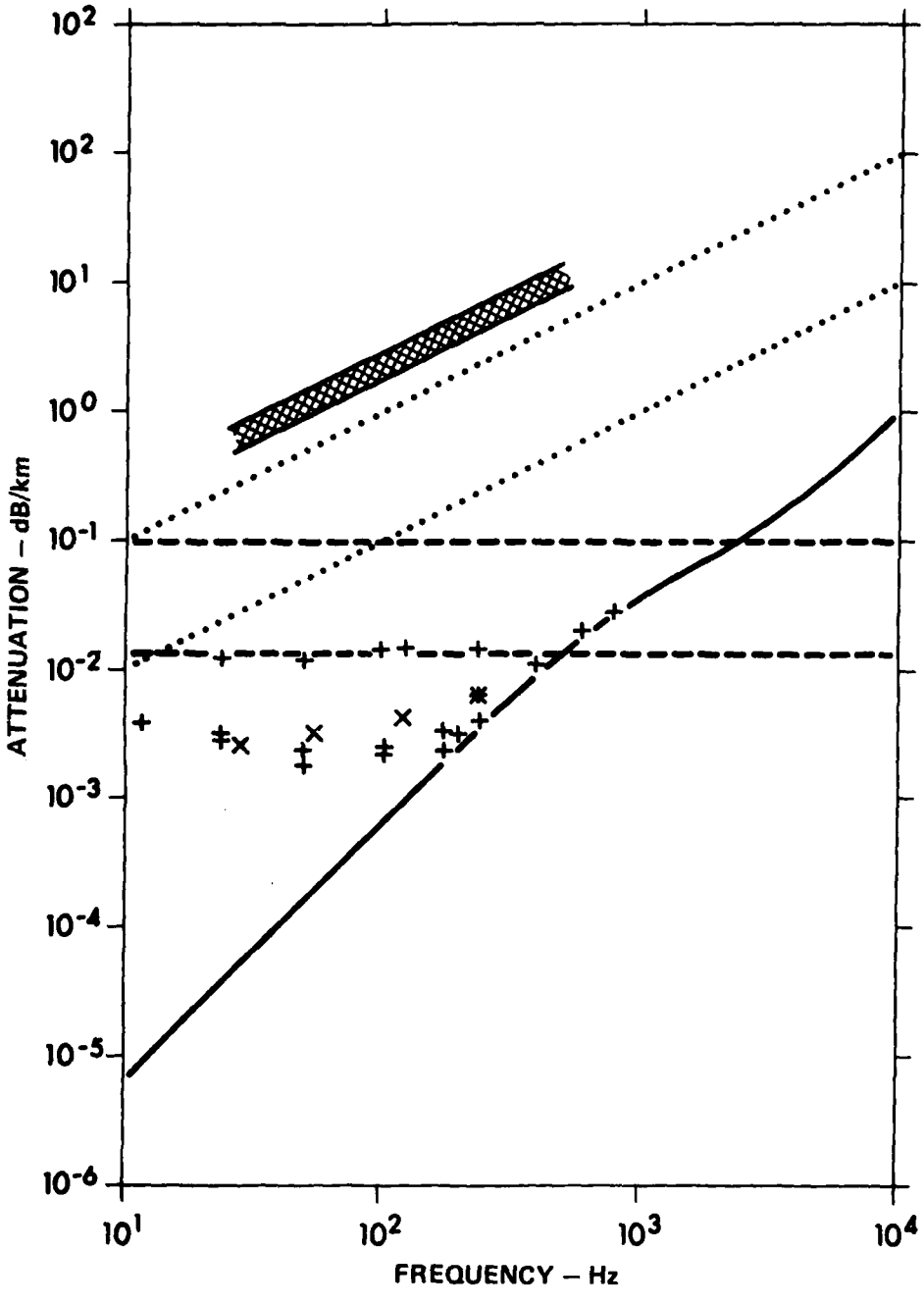

FIGURE 16

COMPARISON OF ATTENUATION VALUES FOR LINEAR FREQUENCY DEPENDENT (...) AND FREQUENCY INDEPENDENT (---) MEASURED SEA WATER ATTENUATIONS (SYMBOLS) AND DEEP SEA SEDIMENTS (SHADED REGION)

THORP CURVE (—) PRESENTED AS A REFERENCE

ARL:UT
AS-81-563
KCF - GA
5 - 22 - 81
REV 8-19-81

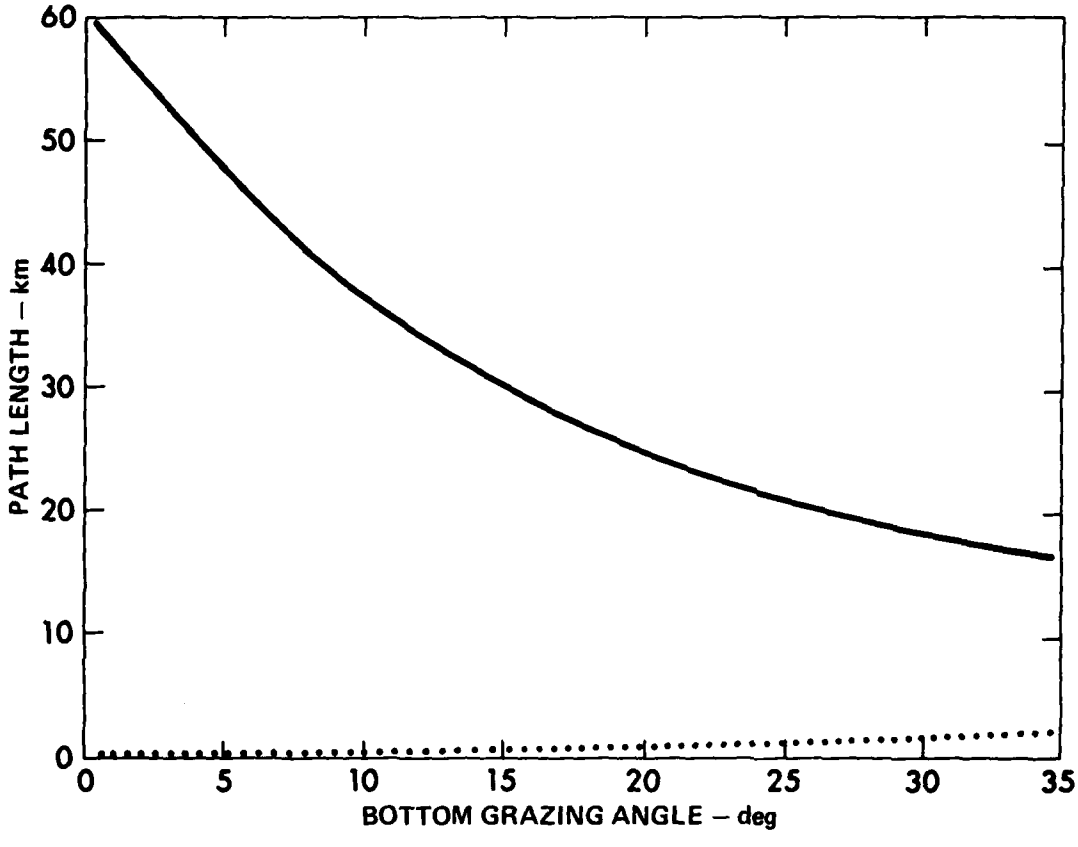

FIGURE 17

PATH LENGTH IN WATER (——) AND IN SEDIMENT (....)
FOR THE SOUND VELOCITY PROFILE SHOWN IN FIG. 9

ARL:UT
AS-81-565
KCF - GA
5 - 22 - 81
REV 8-19-81

REFERENCES

1. A. C. Kibblewhite and L. D. Hampton, "A Review of Deep Ocean Attenuation Data at Very Low Frequencies," J. Acoust. Soc. Am. 67, 147-157 (1980).

2. K. M. Guthrie, "The Propagation of SOFAR Signals," Ph.D dissertation, Department of Physics, The University of Auckland, New Zealand (1974).

3. A. C. Kibblewhite, J. A. Shooter, and S. L. Watkins, "Examination of Attenuation at Very Low Frequencies Using the Deep Water Ambient Noise Field," J. Acoust. Soc. Am. 60, 1040-1047 (1976).

4. Ruth Gonzalez and Kenneth E. Hawker, "The Acoustic Normal Mode Model NEMESIS," Applied Research Laboratories Technical Report No. 80-13 (ARL-TR-80-13), Applied Research Laboratories, The University of Texas at Austin, in preparation.

5. Ruth Gonzalez and Susan G. Payne, "User's Manual for NEMESIS and PLMODE," Applied Research Laboratories Technical Memorandum No. 80-6 (ARL-TM-80-6), Applied Research Laboratories, The University of Texas at Austin, 1 May 1980.

6. Edwin L. Hamilton, "Geoacoustic Modeling of the Sea Floor," J. Acoust. Soc. Am. 68, 1313-1340 (1980).

7. Stephen K. Mitchell and Karl C. Focke, "New Measurements of Compressional Wave Attenuation in Deep Ocean Sediments," J. Acoust. Soc. Am. 67, 1582-1589 (1980).

8. Robert J. Urick, Principles of Underwater Sound (McGraw-Hill Book Co., Inc., New York, 1975), 2nd ed., pp. 96-104.

9. H. F. Bezdek, "Pressure Dependence of Sound Attenuation in the Pacific Ocean," J. Acoust. Soc. Am. 53, 782-788 (1973).

10. M. Schulkin and H. W. Marsh, "Sound Absorption in Sea Water," J. Acoust. Soc. Am. 34, 864-865 (1962).

11. Robert H. Mellen and David G. Browning, "Variability of Low-Frequency Sound Absorption in the Ocean: pH Dependence," J. Acoust. Soc. Am. 61, 704-706 (1977).

12. W. H. Thorp, "Analytic Description of the Low-Frequency Attenuation Coefficient," J. Acoust. Soc. Am. 42, 270 (1967).

6 January 1982

DISTRIBUTION LIST FOR
ARL-TM-82-1
UNDER CONTRACT N00014-80-C-0490
UNCLASSIFIED

Copy No.

Commanding Officer
Office of Naval Research
Arlington, VA 22217
1 Attn: R. Ryan (Code 400R)
2 E. Wegman (Code 436)
3 R. Obrochta (Code 230)
4 CAPT A. Gilmore (Code 200)

5 Office of Naval Research
Branch Office Chicago
Room 286, 536 South Clark St.
Chicago, IL 60605

Commanding Officer
Naval Ocean Research and Development Activity
NSTL Station, MS 39529
6 Attn: E. Chaika (Code 530)
7 L. Solomon (Code 500)
8 S. Marshall
9 R. Gardner
10 G. Morris

Superintendent
Naval Postgraduate School
Monterey, CA 93940
11 Attn: H. Medwin
12 Library

Commanding Officer
Naval Oceanographic Office
NSTL Station, Bay St. Louis, MS 39522
13 Attn: W. Jobst
14 G. Lewis

15 - 26 Commanding Officer and Director
Defense Technical Information Center
Cameron Station, Building 5
5010 Duke Street
Alexandria, VA 22314